Polarization Diversified 4X4 Uniformly Distributed Homogeneous Metasurface Backed MPA

Swarnadipto Ghosh
Department of Avionics
Indian Institute of Space Science and Technology
Thiruvananthapuram, India
swarnadipto.2000@gmail.com

Dipankar Saha
Department of Avionics
Indian Institute of Space Science and Technology
Thiruvananthapuram, India
dipankarsahauem@gmail.com

Ayona Chakraborty
Department of Electronics and Telecommunication Engineering
Jadavpur University
Kolkata, India
ayonachakraborty1@gmail.com

Samik Chakraborty
Department of ECE
Regent Education and Research Foundation
Kolkata, India
chakrasamik@gmail.com

Bhaskar Gupta
Department of Electronics and Telecommunication Engineering
Jadavpur University
Kolkata, India
gupta_bh@yahoo.com

Sunday Cookey Ekpo
Department of Engineering
Manchester Metropolitan University
Manchester, UK.
s.ekpo@mmu.ac.uk

Stephen Alabi
Wilsons Park, Monsall Road
Manchester, M40 8WN, United Kingdom
Stephen.alabi@smopct.com

***Abstract*—In this article, a 4X4 uniformly distributed homogeneous array of subwavelength unit-cell based metasurface backed slotted microstrip patch antennas (MPA) has been proposed to modulate the radiation pattern characteristics and realize polarization diversity. In this proposed dual layer architecture, to analyze the polarization diversification effect on the metasurface layer both the bilinear and orthogonally decomposed surface current vector components have been realized. Achieving circular polarization (CP) in the higher order hybrid or quasi-TEM mode is indicated the orthogonally decomposed surface current vector components through the metasurface. The proposed dual layer metasurface backed MPA architecture can be used in GSM;2.27GHz, WLAN;5.2 GHz and X band;8.78 GHz applications.**

Keywords—Metasurface, dual-layer architecture, polarization diversification, tri-band MPA, metasurface backed MPA

I. INTRODUCTION (*HEADING 1*)

Metamaterial with its unique properties can be used for less real estate occupation [1] – [4]. Khan et.al. in [5] have investigated the challenges of body centric wideband antenna design using metamaterials [6-9] and partial ground plane. Use of partial ground plane invariably gives rise to pattern distortion. A multiband spiral antenna design has been shown in [10] with the requisite study of biocompatible insulation and choice of layers to improve radiation efficiency. EBG and SRR has been introduced by Wajid et. al. [11] in a wearable dual band antenna wherein the effect of the cotton substrate material on the gain of the antenna has been explicitly probed. In [12][13] 5G biomedical applications has been shown. In [13] CPW feed has been introduced to aid for compactness which may give rise to design complications. Graphene owing to its high electrical conductivity has been used for a reconfigurable antenna design [14] in terahertz frequency. Here use of graphene raises the material cost and design complications; moreover, in THz frequencies there is a restriction of communication range. A relatively larger metasurface backed circularly polarized (CP) antenna has been reported by Kam et.al[15].

In the present work, a dual stacked 4X4 array of subwavelength meta unit-cell surface backed MPA has been reported. This work consists of CP in all the higher order hybrid modes and having dual polarized nature in fundamental mode of resonance. Sections II and III consist of design and analysis of the dual stacked proposed antenna.

II. DESIGN STAGES OF PROPOSED ANTENNA

This article proposes a dual layer microstrip patch antenna (MPA) architecture by using a subwavelength meta unit-cell backed slotted MPA.

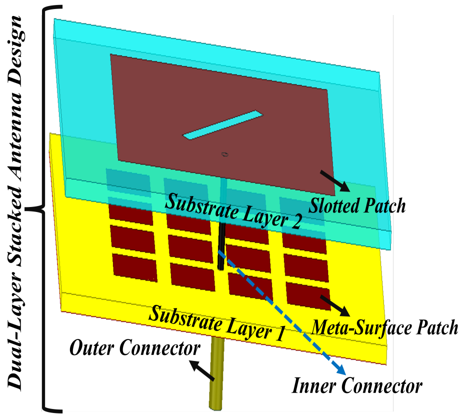

Fig.1. Schematic of Dual-Layer architecture of the proposed antenna excited through co-axial connector

The dual layer architecture has been achieved by stacking two layers of Teflon dielectric substrate having permittivity (ϵ_r=2.4) and loss tangent (tan δ=0.0009).

A slotted microstrip patch (MP) has been printed on the upper dielectric layer whereas the 4X4 array of subwavelength meta unit cell structure has been printed on the lower dielectric layer followed by a ground plane on the other side of the lower dielectric substrate.

As showing from Fig.1, the rectangular slotted MP has been excited through a co-axial feed connected through the ground layer of the lower substrate up to the surface layer of the slotted MP. If outer radius of the coaxial connector is $r_{co-ax(out)}$ =1.2 mm while the inner radius is $r_{co-ax(in)}$=

0.6mm.

The detailed layered architecture has been shown throughout Fig.2. Fig.2 indicates the overall dimension of the substrate is (L_gXW_g) =(*60mmX60mm*) whereas the MP printed on the upper dielectric substrate has a dimension of (L_pXW_p)=(*20mmX20mm*). The dimension of the electrical slot upon the printed MP (L_sXW_s)=(*12mmX2mm*) are rotated by an angle θ=*45°*.

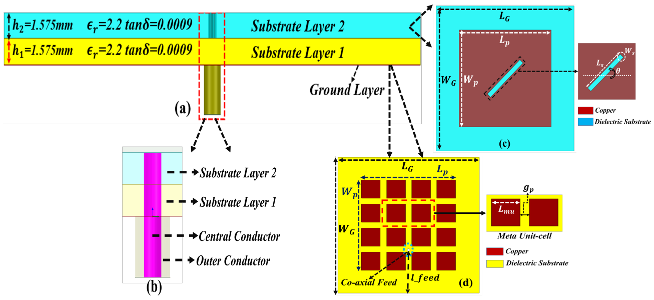

Fig.2. Schematic representation of Dual-Layer architecture of the proposed antenna excited through co-axial connector : (a) side view of the stacked dielectric structure (b) co-axial feed connector (c) top view of rectangular slotted microstrip patch (MP) printed on upper dielectric substrate (d) top view of the 4X4 array of subwavelength meta unit-cell printed on top portion of lower dielectric substrate.

Also, each subwavelength meta unit-cell has a dimension of ($L_{mu}XL_{mu}$)=(*8mmX8mm)* which has been chosen on the basis of operating frequency (f_r)=*2.4 GHz* and mapped to at least $\frac{\lambda}{15}$ for realizing the actual physical behavior of subwavelength structures. The interelement gap is defined as g_p=*2.66mm*. Ground layer, microstrip patch (MP) and the 4X4 array of subwavelength meta unit cell structure have all been considered as perfect electric conductors (PEC).

III. Performance Analysis of Proposed Antenna

In this section, a comparative analysis (mentioned in *Fig. 3*) between the single and dual layer 4X4 subwavelength meta unit-cell array backed slotted microstrip patch antenna (MPA) is presented.

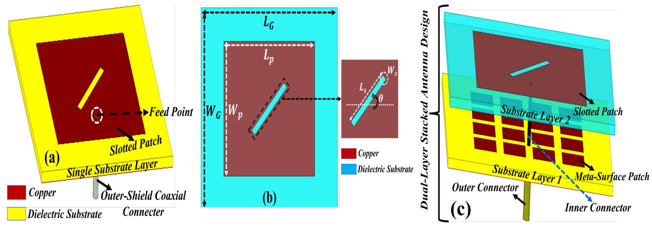

Fig.3. Comparison of single and dual layer architecture (a) single layer 3D architecture for slotted MPA with co-axial feed excitation (b) top view of slotted MP (c) dual layer stacked proposed antenna architecture.

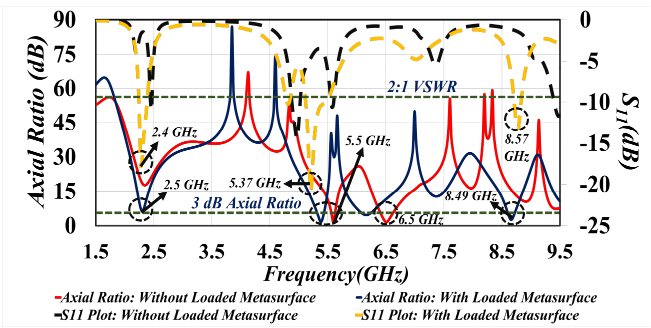

Fig.4. Simulated *S_{11}(dB)* and *Axial Ratio (dB)* plot for both with and without loading of 4X4 array of subwavelength array of meta unit-cell surface.

To study the electromagnetic behavior of the subwavelength 4X4 array of meta unit-cell surface, it has been placed as an intermediate ground plane in the stacked form of two dielectric substrates. The meta-surface shown in Fig. 3(c) is behaving like a periodic defected ground structure (*DGS*) having magnetic boundary bounded by electric walls periodically. Modulation of the effective surface wave through the meta-surface boundary by periodic modulation of phase velocity (v_p) and group velocity (v_g) has been depicted in this section of this article.

It is shown in the next sub-sections that how the wave-vector has been modulated for the periodically loaded subwavelength patches due to the inter-patch gap which can exhibit parasitic capacitances and give coupling effects for subwavelength electromagnetic applications.

In Fig.4 the simulated *S_{11}(dB)* and *Axial Ratio(dB)* for both with and without 4X4 array of subwavelength array of meta unit-cell surface loading are compared. It is clearly visible from Fig.4 that for both with and without meta-surface loaded MPA structures the fundamental TM_{01} has been excited at *2.4 GHz*. Along with the fundamental mode of resonance, higher order *quasi-TEM* and hybrid modes have been generated. For the proposed 4X4 array of subwavelength meta unit-cell loaded surface backed, three frequencies in S, C and X band region are identified which have effective *S_{11}(dB)<-10dB*.The proposed meta-surface backed MPA can be operated in centering around the three bands such as *2.4GHz*,*5.37 GHz* and *8.57 GHz*. Also, it can be observed from the axial ratio plot of Fig.4, the MPA without the 4X4 array of meta unit-cell surface backing isn't circularly polarized at the desired operating bands. After the 4X4 array of meta unit-cell surface backing under the slotted MPA is introduced. It can be observed from the axial ratio plot that for the fundamental resonance mode axial ratio(dB)< *5.5dB* whereas the other higher *order quasi-TEM* modes exhibit axial ratio(dB)< *2.8 dB* in each band. So, it can be arranged that the 4X4 array of meta unit-cell surface backing reduces the overall cross polar radiation. The bilinear surface current distribution has been replaced through orthogonal vector current distributions. The vector surface current distribution on the meta-surface patch and the slotted MP can give a clear indication on the polarization diversity.

From Fig.5 how the surface current components have been modulated for the slotted MPA while backing with the 4X4 array of subwavelength meta unit-cell surface as a periodically defected PEC surface can be explained. It can be observed that at lower frequency band (*2.46 GHz*) the dual polarization is detained due to the complementary excitation of the magnetic boundary which is realized by the electrical slot on the PEC microstrip patch (MP). On the other hand, for mid and upper band (*4.97 GHz & 5.56 GHz*) frequencies it can be clearly observed that due to linear excitation of the electrical slot it exhibits linear polarization in each band which can be verified from the axial ratio plot for the bands (mentioned in Fig 4).

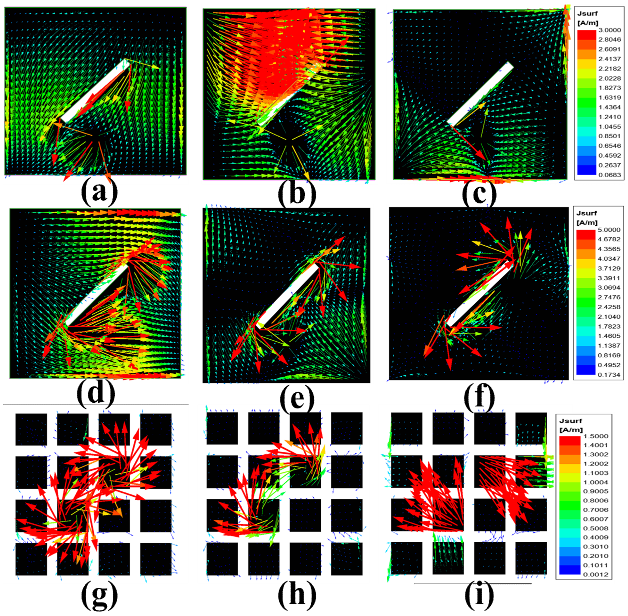

Fig.5. Surface Current Vector plot of slotted MP without Metasurface backing at (a) 2.46 GHz (b) 4.97 GHz (c) 5.56 GHz, with Metasurface backing at (d) 2.4 GHz (e) 5.27 GHz (f) 8.78 GHz, Surface Current plot of 4X4 array of subwavelength meta unit-cell surface at (g) 2.4 GHz (h) 5.56 GHz (i) 8.78 GHz

It can be observed from the surface current distribution that for each frequency band (*2.4 GHz,4.97 GHz,8.78 GHz*) the complementary effect of the electrical slot excitation has been occurred which causes dual polarization in the lower frequency band (*2.4 GHz*) and strong circular polarization in both middle and upper frequency bands (*5.27 GHz & 8.78 GHz*). The above statement can be verified by the axial ratio plot shown in Fig. 4.

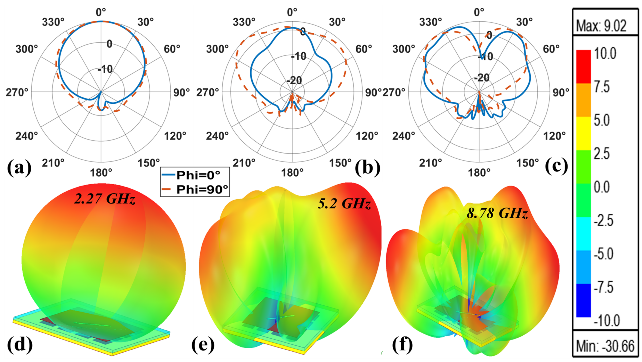

Fig.6. 2D radiation patterns for Single layering Antenna at (a) 2.46 GHz (b) 4.97 GHz (c) 5.56 GHz along with corresponding 3D radiation patterns at (d) 2.46 GHz (e) 4.97 GHz (f) 5.56 GHz

By observing the surface current in the respective frequency bands, it can be observed that by applying the periodically defected subwavelength meta unit-cell loaded PEC structure on the back side of the slotted MP, the fundamental resonance mode is restricted to dual polarization whereas the higher order quasi-TEM or hybrid resonance modes exhibit complete circular polarization for the periodic loading effect on phase and group velocities at those frequencies.

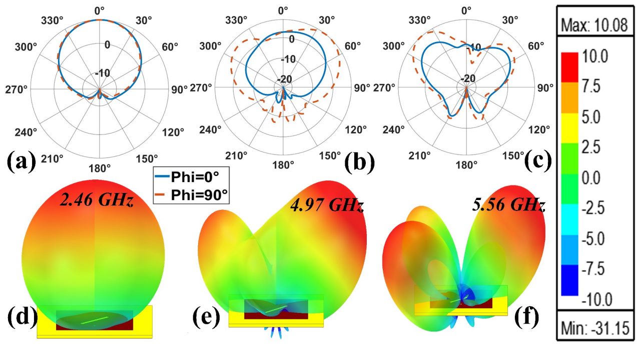

Fig.7. 2D radiation patterns for Dual layer 4X4 array of subwavelength meta unit-cell surface backed Antenna at (a) 2.46 GHz (b) 4.97 GHz (c) 5.56 GHz along with corresponding 3D radiation patterns at (d) 2.46 GHz (e) 4.97 GHz (f) 5.56 GHz

From the Figs.5(g)-(i), it can be understood that at the dual polarization band the consecutive PEC loaded patches have been coupled through a mixed effect of orthogonal and bilinear excitations whereas for the remaining hybrid modes, the circular polarization exhibits orthogonal or 90° phase coupled effects.

From Fig.6, both 2D and 3D radiation pattern for microstrip patch antenna (MPA) structure exhibit that for fundamental mode resonance the undistorted hemispherical regular shaped pattern has been obtained whereas the higher order hybrid or quasi-TEM mode of resonance exhibit doughnut shaped dual or multibeam pattern with a sustainable max-gain of 10.02 dBi. Similarly from Fig.7, it can be seen that undistorted hemispherical regular shaped radiation pattern has been achieved at the lowest order mode of resonance while for higher order hybrid modes doughnut shaped dual or multibeam pattern having broadside null has been achieved with a sustainable max gain of 9.02 dBi showing circular polarization (CP) effect. All the higher order bands which exhibit dual or multibeam radiation pattern can be used for bidirectional or multi beam communication applications.

As a use case scenario, current vehicle-to-anything (V2X) applications include the use of existing cellular or 802.11x-based technology which employs the use of conventional beamforming multiple input multiple output (MIMO) techniques to optimise spectral efficiency [16-17]. Although in theory, current beamforming MIMO techniques and technologies allow for higher capacity and throughput, practical systems have showed disappointing results, especially with regards to range, performance and cost of implementation in multiple user MIMO (MU-MIMO) or massive MIMO – as the technique requires users to be sufficiently separated for an optimal performance. Other beamforming techniques rely heavily on phase shifting, which requires active amplification to accomplish beam-steering at a suitable level. Although phased array systems in hybrid-MIMO systems would be able to provide somewhat decent throughput at a reduced cost and power consumption compared with traditional MIMO systems, this approach becomes too costly and thermal challenges arise as it is scaled-up [18]. Moreover, when employing the use of mmWave 5G-satellite convergence ecosystem [19], the benefits of MIMO are diminished if an object is moving too fast due to rapid channel evolution, such as in vehicles. In terms of V2X applications, the very nature of the application is that there will always be multiple high-frequency connections between a vast number of vehicles, all moving at different speeds and all at varying distances. In mmWave-based V2X implementations and beyond, beamforming metasurfaces, which are software-defined, provide the potential to overcome problems with SWaP-C requirements [20], and thermal management.

IV. Conclusion

In this article a detailed characterization of the proposed dual band stacked 4X4 array of subwavelength meta unit-cell surface backed MPA architecture has been presented. The electromagnetic effect of the periodically defected partial ground structure has been reported. The proposed antenna structure can be used for short-range biomedical communication, implantable sensing applications.

References

[1] Raghavan, S., and V. Rajeshkumar. "An overview of metamaterials in biomedical applications." Prog. Electromagn. Res 25 (2013): 369.

[2] Jamlos, Mohd Aminudin, Nur Amirah Othman, Wan Azani Mustafa, and Maswani Khairi Marzuki. "Metamaterial Antenna for Biomedical Application." In Proceedings of the 11th National Technical Seminar on Unmanned System Technology 2019: NUSYS'19, pp. 519-528. Springer Singapore, 2021.

[3] Keltouma, Nouri, Saidi Amaria, Becharef Khadidja, Chikhi Mokhtaria, Seghier Salima, Becharef Kada, and Abes Turkiya. "Dual-Band Half-Circular Ring Implantable Antenna With Metamaterial SRR For Biomedical Applications." Telecommunications and Radio Engineering 82, no. 3 (2023).

[4] Naik, Ketavath Kumar, Seelam Chaithanya Satya Teja, Bokkisam Venkata Sailaja, and Pasumarthi Amala Sri. "Design of flexible parasitic element patch antenna for biomedical application." Progress In Electromagnetics Research M 94 (2020): 143-153.

[5] Khan, Umhara Rasool, Javaid A. Sheikh, Shahid Bashir, and Suhaib Ahmed. "Metamaterial inspired wideband on-body antenna design for bio-medical applications." Materials Today: Proceedings 80 (2023): 1772-1776.

[6] Z. Wang, J. Liu, and Y. Long, "A simple wide-bandwidth and highgain microstrip patch antenna with both sides shorted," IEEE Antennas Wireless Propag. Lett., vol. 18, no. 6, pp. 1144–1148, Jun. 2019.

[7] S. X. Ta and I. Park, "Compact wideband circularly polarized patch antenna array using metasurface," IEEE Antennas Wireless Propag. Lett., vol. 16, pp. 1932–1936, 2017. [6] Y. Cao et al., "Broadband and high-gain microstrip patch antenna loaded with parasitic mushroom-type structure," IEEE Antennas Wireless Propag. Lett., vol. 18, no. 7, pp. 1405–1409, Jul. 2019.

[8] W. Liu, Z. N. Chen, and X. Qing, "Metamaterial-based low-profile broadband aperture-coupled grid-slotted patch antenna," IEEE Trans. Antennas Propag., vol. 63, no. 7, pp. 3325–3329, Jul. 2015.

[9] Malik, Nabeel Ahmed, Paul Sant, Tahmina Ajmal, and Masood Ur-Rehman. "Implantable antennas for bio-medical applications." IEEE Journal of Electromagnetics, RF and Microwaves in Medicine and Biology 5, no. 1 (2020): 84-96.

[10] Wajid, Abdul, Ashfaq Ahmad, Sadiq Ullah, Dong-you Choi, and Faiz Ul Islam. "Performance Analysis of Wearable Dual-Band Patch Antenna Based on EBG and SRR Surfaces." Sensors 22, no. 14 (2022): 5208.

[11] Sabban, Albert. "Wideband wearable antennas for 5G, IoT, and medical applications." In Advanced Radio Frequency Antennas for Modern Communication and Medical Systems. London, UK: IntechOpen, 2020.

[12] Butt, Arslan Dawood, Jalal Khan, Sarosh Ahmad, Adnan Ghaffar, Ahmed Jamal Abdullah Al-Gburi, and Mousa Hussein. "Single-fed broadband CPW-fed circularly polarized implantable antenna for sensing medical applications." Plos one 18, no. 4 (2023): e0280042.

[13] Sathiyapriya, T., T. Poornima, and R. Sudhakar. "Design and Characterization of Novel Reconfigurable Graphene Terahertz Antenna Using Metamaterials." Advances in Terahertz Technology and Its Applications (2021): 253-272.

[14] Andrei Andryieuski and Andrei V. Lavrinenko, "Graphene metamaterials based tunable terahertz absorber: effective surface conductivity approach," Opt. Express 21, 9144-9155 (2013)

[15] Koohestani, Mohsen, and Alireza Ghaneizadeh. "An ultra-thin double-functional metasurface patch antenna for UHF RFID applications." *Scientific Reports* 11, no. 1 (2021): 1-14.

[16] S. C. Ekpo, "Parametric System Engineering Analysis of Capability-Based Small Satellite Missions," in IEEE Systems Journal, vol. 13, no. 3, pp. 3546-3555, Sept. 2019, doi: 10.1109/JSYST.2019.2919526.

[17] S. C. Ekpo, B. Adebisi and A. Wells, "Regulated-Element Frost Beamformer for Vehicular Multimedia Sound Enhancement and Noise Reduction Applications," in IEEE Access, vol. 5, pp. 27254-27262, 2017, doi: 10.1109/ACCESS.2017.2775707.

[18] Ekpo, Sunday C., Bamidele Adebisi, and Andrew Wells. "Regulated-element frost beamformer for vehicular multimedia sound enhancement and noise reduction applications." *IEEE Access* 5 (2017): 27254-27262.

[19] M. Zafar, S. Ekpo, J. George, P. Sheedy, M. Uko and A. Gibson, "Hybrid Power Divider and Combiner for Passive RFID Tag Wireless Energy Harvesting," in IEEE Access, vol. 10, pp. 502-515, 2022, doi: 10.1109/ACCESS.2021.3138070.

[20] S. C. Ekpo and D. George, "Impact of Noise Figure on a Satellite Link Performance," in IEEE Communications Letters, vol. 15, no. 9, pp. 977-979, September 2011, doi: 10.1109/LCOMM.2011.072011.111073.